

Experimental (FT-IR, FT-Raman, UV-Vis, ^1H and ^{13}C NMR) and computational (density functional theory) studies on 3-bromophenylboronic acid



M. Karabacak^a, E. Kose^b, A. Atac^b, E.B. Sas^c, A.M. Asiri^{d,e}, M. Kurt^{c,*}

^a Department of Mechatronics Engineering, H.F.T. Technology Faculty, Celal Bayar University, Turgutlu, Manisa, Turkey

^b Department of Physics, Celal Bayar University, Manisa, Turkey

^c Department of Physics, Faculty of Art and Science, Ahi Evran University, Kırşehir, Turkey

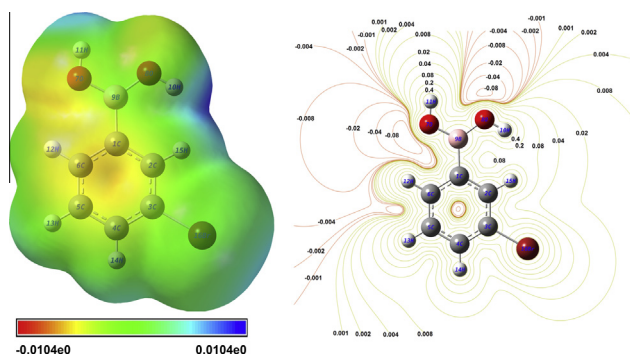
^d Department of Chemistry, Faculty of Science, King Abdulaziz University, Jeddah, Saudi Arabia

^e Center of Excellence for Advanced Materials Research, King Abdulaziz University, Jeddah, Saudi Arabia

HIGHLIGHTS

- Monomeric conformations and dimeric structure of 3-bromophenylboronic acid were investigated.
- The compound was characterized by FT-IR, FT-Raman, NMR and UV spectroscopy.
- The vibrational frequencies, chemical shifts and electronic absorption wavelengths were calculated by DFT.

GRAPHICAL ABSTRACT



ARTICLE INFO

Article history:

Received 10 April 2014

Received in revised form 21 July 2014

Accepted 22 July 2014

Available online 1 August 2014

Keywords:

3-Bromophenylboronic acid

FT-IR and FT-Raman spectra

UV-Vis and NMR spectra

HOMO-LUMO

Density of state

ABSTRACT

Structurally, boronic acids are trivalent boron-containing organic compounds that possess one alkyl substituent (i.e., C-Br bond) and two hydroxyl groups to fill the remaining valences on the boron atom. We studied 3-bromophenylboronic acid (3BrPBA); a derivative of boronic acid. This study includes the experimental (FT-IR, FT-Raman, ^1H and ^{13}C NMR, UV-Vis) techniques and theoretical (DFT-density functional theory) calculations. The experimental data are recorded, FT-IR (4000–400 cm^{-1}) and FT-Raman spectra (3500–10 cm^{-1}) in the solid phase. ^1H and ^{13}C NMR spectra are recorded in DMSO solution. UV-Vis spectrum is recorded in the range of 200–400 nm for each solution (in ethanol and water). The theoretical calculations are computed DFT/B3LYP/6-311++G(d,p) basis set. The optimum geometry is also obtained from inside for possible four conformers using according to position of hydrogen atoms after the scan coordinate of these structures. The fundamental vibrations are assigned on the basis of the total energy distribution (TED) of the vibrational modes, calculated with scaled quantum mechanics (SQM) method and parallel quantum solutions (PQS) program. ^1H and ^{13}C NMR chemical shifts are tracked on by using the gauge-invariant atomic orbital (GIAO) method. The time-dependent density functional theory (TD-DFT) is used to find HOMO and LUMO energies, excitation energies, oscillator strengths. The density of state of the studied molecule is investigated as total and partial density of state (TDOS and PDOS) and overlap population density of state (OPDOS or COOP) diagrams have been presented. Besides, frontier molecular orbitals (FMOs), molecular electrostatic potential surface (MEPs) and thermodynamic proper-

* Corresponding author. Tel.: +90 386 211 45 54; fax: +90 386 252 80 54.

E-mail address: kurt@gazi.edu.tr (M. Kurt).

ties are performed. At the end of this work, the results are ensured beneficial for the literature contribution.

© 2014 Elsevier B.V. All rights reserved.

Introduction

Boronic acids are not naturally occurring, though they have appeared in the literature since at least 1860 [1]. Unique, versatile reactivity and stability of boronic acids have led to uses in numerous areas, including C–C bond formation, acid catalysis, asymmetric synthesis, carbohydrate analysis, metal-catalysis, molecular sensing, and as therapeutic agents, enzyme inhibitors, and novel materials [2–4]. Boronic acids and wide types of derivatives are far-going many areas; material science, supra-molecular chemistry, analytical chemistry, medicine, biology, catalysis, organic synthesis and crystal engineering and used as reagents with in organic synthesis, enzyme inhibitors, catalysts, protecting groups, and affinity purification agents, receptors for saccharide sensing, neutron capturing agents for cancer therapy, bio conjugates, and protein labels [5].

Identify carbohydrates that are potentially suitable linear linkers—in both a geometrical and a chemical sense—for linear and higher dimensional boronic acid nodes were reported [6]. O'Donovan et al. [7] concluded a novel class of bacterial of boronic acids mutagen that may not act by direct covalent binding to DNA. Biomedical applications of boronic acid-containing polymers and biological of particular dichlorophenylboronic acids were studied [8–10]. The moiety of boronic acids was incorporated into nucleosides and amino acids as antiviral agents and anti-tumor [11]. Also their derivatives of divergent biologically important compounds have been synthesized as anti-metabolites for a possible two-pronged attack on cancer [12–14].

Phenylboronic acid is containing a phenyl substituent and two hydroxyl groups attached to boron. The molecular structures of phenylboronic acid and its derivatives were studied many authors. Infrared spectra of phenylboronic acid and diphenyl phenylboronate were studied by Faniran [15]. Rettig and Trotter studied crystal and molecular structure of phenylboronic acid [16]. Cyrański et al. [17] analyzed the molecular structures of phenylboronic acid and its dimer using X-ray structural analysis and spectroscopic methods. The crystal structures of 3-fluorophenylboronic acid and 2,4-difluorophenylboronic acid were identified by Wu et al. [18] and Rodriguez et al. [19], respectively. Shimpi et al. [20] reported the crystal structures of 4-chloro- and 4-bromophenylboronic acids and hydrates of 2- and 4-iodophenylboronic acid in two different forms, which were characterized by single-crystal X-ray diffraction methods. The molecular and crystal structures of 3-Formylphenylboronic acid [21] and 3-aminophenylboronic acid monohydrate [22] were analyzed.

DFT calculations are reported to provide excellent vibrational frequencies of organic compounds if the calculated frequencies are scaled to compensate for the approximate treatment of electron correlation, for basis set deficiencies and for the anharmonicity [23–27].

Literature survey reveals that there are theoretical and spectroscopic studies regarding on the boronic acid and its derivatives. The molecular structure and vibrational spectra of the 4-chloro- and 4-bromophenylboronic acids [28], pentafluorophenylboronic acid [29], 3,5-dichlorophenylboronic acid [30], 3,4-dichlorophenylboronic acid [31], 2,4- and 2,6-dimethoxyphenylboronic acid [32,33] and also 3- and 4-pyridineboronic acid molecules [34] were reported theoretically and experimentally. Erdogdu et al. [35] presented the theoretical and experimental analysis of 2-fluor-

ophenylboronic acid. Moreover, the experimental and theoretical investigation of the conformation, vibrational and electronic transitions of 2,3-difluorophenylboronic acid molecule [36] and acenaphthene-5-boronic acid [37] were studied. Rani et al. [38] set out experimental and theoretical investigation of the conformation, vibrational and electronic transitions of methylboronic acid.

To the best of our knowledge showed that, there is no theoretical (DFT) and experimental spectroscopic studies performed on the conformational, vibrational (IR and Raman), NMR and UV–Vis spectra about on monomer and dimer structures of 3BrPBA. This insufficiency encourages us to represent the detailed description of 3BrPBA experimentally (FT-IR, FT-Raman, ^1H and ^{13}C NMR, and UV–Vis spectra) and theoretically (DFT). In addition we investigated the heat capacity, entropy, and enthalpy of the title molecule according to the different temperatures. The nonlinear optical properties (NLO) of the studied molecule are represented, addressed on theoretical calculations.

Experimental

The 3BrPBA ($\text{C}_6\text{H}_4\text{BrB}(\text{OH})_2$) molecule was provided from Across Organics Company in solid state with a stated purity of 97% and it was used as no extra purification. FT-IR, FT-Raman, NMR and UV–Vis spectra of the title molecule are performed as described the following sentences. FT-IR spectrum of the compound is recorded between 4000 and 400 cm^{-1} on a Perkin–Elmer FT-IR System Spectrum BX spectrometer by using a KBr disc technique. The spectrum was recorded at room temperature, with a scanning speed of 10 $\text{cm}^{-1} \text{min}^{-1}$ and the spectral resolution of 4.0 cm^{-1} . FT-Raman spectrum of the 3BrPBA molecule is recorded in the region 3500–10 cm^{-1} on a Bruker RFS 100/S FT-Raman instrument using 1064 nm excitation from an Nd:YAG laser. The detector is a liquid nitrogen cooled Ge detector. Five hundred scans were accumulated at 4 cm^{-1} resolution using a laser power of 100 mW. The ^1H and ^{13}C NMR spectra of the headline molecule are carried out in Varian Infinity Plus spectrometer at 300 K, dissolved in DMSO. The chemical shifts are reported in ppm relative to tetramethylsilane (TMS) for ^1H and ^{13}C NMR spectra. Last one, the UV–Vis spectrum of the title molecule, solved in ethanol and water, is registered in the range of 200–400 nm using Shimadzu UV-2101 PC, UV–Vis recording Spectrometer. The results are analyzed by UV PC personal spectroscopy software, version 2.33.

Computational details

In the last years, considerable effort has been directed to the understanding of organic molecule of theoretical calculations with the DFT [39] with the Becke's three-parameter hybrid functional (B3) [40], for the exchange part and the Lee–Yang–Parr (LYP) correlation function [41], accepted as a cost-effective approach. We have utilized this theory for the computation of molecular structure, vibrational frequencies, chemical shifts and energies of optimized structures. In this connection, in the ground state theoretical geometrical parameters, IR, Raman, (^1H and ^{13}C) NMR and UV–Vis spectra of the studied molecule were calculated by dint of Gaussian 09 suite of quantum chemical codes [42].

The first task to find the most stable structure of the title molecule within four possible conformers were proposed as named

trans-cis (TC), *cis-trans* (CT), *trans-trans* (TT) and *cis-cis* (CC). Then the selected torsion angle $T(O-B-C)$, is changed every 10° and molecular energy profile is calculated from 0° to 180° and optimized by using the hybrid B3LYP level of theory in DFT with the 6-311++G(d,p) basis set [40,41] for all proposed conformers. The optimized structural parameters are used in the vibrational frequencies, isotropic chemical shifts and calculations of electronic properties. The harmonic frequencies are multiplied by scaled factors to obtain the best agreement results with the experimental data. We used the scaling factors as 0.958 for greater and 0.983 smaller than 1700 cm^{-1} , respectively. [43]. The TED of fundamental vibrational modes is calculated by using the SQM method and PQS program [44,45]. The ^1H and ^{13}C NMR isotropic shielding are carried through the GIAO method [46,47] using the optimized parameters obtained from B3LYP/6-311++G(d,p) method. The UV-Vis spectrum, electronic transitions, vertical excitation energies, absorbance and oscillator strengths of the headline molecule are calculated with the TD-DFT.

To analysis group contributions of molecular orbitals and to plot the TDOS (or DOS), PDOS and OPDOS (or COOP) diagrams, GaussSum 2.2 [48] was run on. The OPDOS and PDOS spectra are achieved by convoluting the molecular orbital information with Gaussian curves of unit height and a FWHM (Full Width at Half Maximum) of 0.3 eV. The MEPs of the 3BrPBA and statistical thermodynamic functions (the heat capacity, entropy, and enthalpy) of the molecule are calculated by using from B3LYP/6-311++G(d,p) method. DFT results have also been used to calculate the dipole moment, mean polarizability and first static hyperpolarizability based on the finite field approach.

Results and discussion

3BrPBA molecule has two substituents, $B(OH)_2$ group and Br (bromine) atom is at *meta*-position. Due to model system $B(OH)_2$, dependent on the positions of the hydrogen atoms (bonded to oxygen), whether they are directed away from or toward the ring, provide us to investigate plausible structures (as conformers) of the title molecule. There are four conformers/isomers, had reasonable structure TC, CT, TT and CC are investigated (Fig. 1). Additionally, to explain conformational features of 3BrPBA a conformation analysis was performed between phenyl ring and $B(OH)_2$ group system.

Potential energy surface (PES) scan and energetics

In order to determine conformational flexibility of the caption molecule, the energy profile of the four (TC/CT conformers have the same scan) proposed conformers as a function of $T(O_8-B_9-C_1-C_2)$, torsion angle is varied from 0° to 180° by changing every 10° by using B3LYP/6-311++G(d,p) method. Namely, potential energy curve is calculated by means of scanning $B(OH)_2$ groups

made over the phenyl ring for proposed four conformers. The conformational energy profile shows one local minima near 0° (or 180°) $T(O_8-B_9-C_1-C_2)$ torsion angles for TC/CT and TT conformers, however the CC conformer shows a local minimal cavity at the near 30° (or 150°) given Fig. S1. It is clear from Fig. S1, the conformer (TC) was more stable for 0° (or 180°) torsion angle of the 3BrPBA molecule. All the proposed structures and results of their scans suggest that the TC conformer of the molecule had been the most stable structure.

The energies of proposed (based on the location of hydrogen atom of the molecule and then scan results) different conformations of the title molecule are optimized DFT/B3LYP/6-311++G(d,p) for C_1 and C_s point group symmetries. These calculations are unveiled that TC form is the more stable conformer than the other conformers. TC and TT conformers have positive frequency, while CT and CC conformers have negative frequency for C_s point group symmetry. Therefore using the reference point [the lowest energy (C_s group symmetry of TC)], the relative energy of the other conformers: $\Delta E = E(C_n) - E(C_{TC})$, the energies and energy difference of 3BrPBA molecule were determined in Table 1. The most stable conformer TC has energy differing from by value 0.0516–4.1903 kcal/mol than the other conformers of the heading molecule for C_s group symmetry. Because of TC is the most stable conformer, the discussion below refers only for TC (C_s symmetry) conformer. The geometric parameters (bond lengths and bond angles), vibrational frequencies, NMR chemical shifts and UV-Vis absorption spectra of the studied molecule (TC conformer) are reported by using B3LYP/6-311++G(d,p) with the comparing experimental results.

Geometrical structures

We used the crystal structure of structurally similar phenylboronic acid, 3-fluorophenylboronic acid and 4-bromophenylboronic acid [16,18,20], because of not available in the literature of the 3BrPBA molecule, till now. The geometric parameters are compared with these results [16,18,20]. All conformations of the 3BrPBA with its atomic numbering schemes are shown in Fig. 1. The atomic numbering scheme of dimer TC form of the 3BrPBA molecule is shown in Fig. 2. The optimized geometry parameters, in accordance with the atom numbers of Fig. 1, of monomer and dimer structures of the TC conformer and four possible conformers of 3BrPBA molecule are given in Table S1. It is seen from Table S1 that the theoretical computations are slightly overestimate bond lengths, bond angles from experimental results [16,18,20]. These discrepancies of the molecular geometry between gases phase (theoretical) and solid phase (experimental), owing to extended hydrogen bonding and stacking interactions, are appropriate.

The C–C and C–H bond lengths of the 3BrPBA molecule are approximately equal to for experimental values of phenylboronic

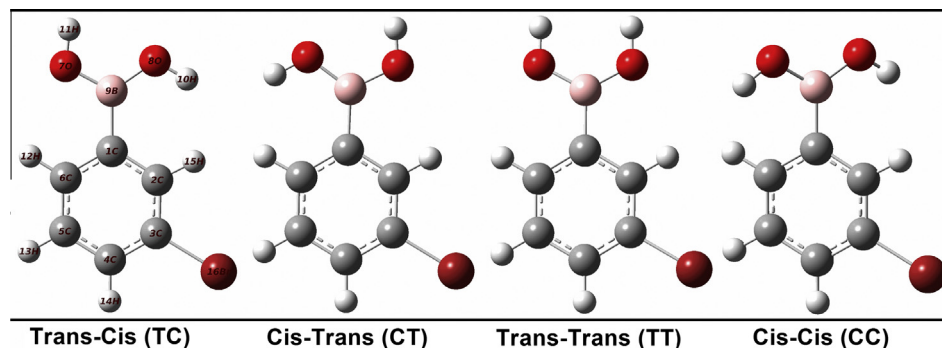
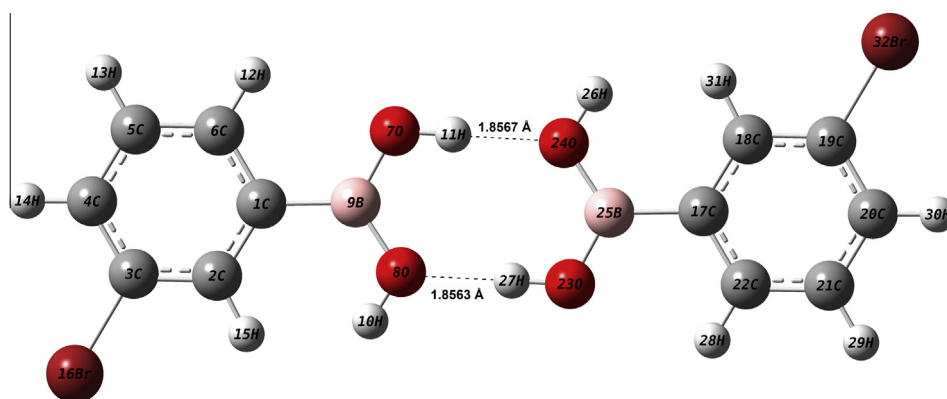


Fig. 1. The theoretical optimized geometric structures (TC, CT, TT and CC conformers) of the 3BrPBA.

Table 1

The calculated energies and energy differences for four possible conformers of 3BrPBA for two group symmetry by using DFT (B3LYP 6-311++G(d,p)) method.

Conformers	Energy		Energy differences ^a		Dipole moment (Debye)	Imaginary frequencies
	(Hartree)	(kcal/mol)	(Hartree)	(kcal/mol)		
<i>C₁</i> group symmetry						
Trans–Cis (TC)	–2981.93795872	–1871194.3975	0.0000	0.0000	0.6753	–
Cis–Trans (CT)	–2981.93787603	–1871194.3456	0.0001	0.0519	2.8609	–
Trans–Trans (TT)	–2981.93505789	–1871192.5772	0.0029	1.8203	3.8253	–
Cis–Cis (CC)	–2981.93260325	–1871191.0369	0.0054	3.3606	2.7188	–
<i>C_s</i> group symmetry						
Trans–Cis (TC)	–2981.93793685	–1871194.3838	0.0000	0.0137	0.6225	–
Cis–Trans (CT)	–2981.93787654	–1871194.3459	0.0001	0.0516	2.8660	–15.17 cm ^{–1}
Trans–Trans (TT)	–2981.93506365	–1871192.5808	0.0029	1.8167	3.8218	–
Cis–Cis (CC)	–2981.93128100	–1871190.2072	0.0067	4.1903	2.8712	–80.86 cm ^{–1}

^a Energies of the other conformers relative to the most stable TC conformer.**Fig. 2.** The theoretical optimized geometric dimer structure of TC conformer of the 3BrPBA.

acid, 3-fluorophenylboronic acid and 4-bromophenylboronic acid [16,18,20]. For example, the C–C bond lengths were observed in the range of 1.365–1.406 Å for 3-fluorophenylboronic acid [18], and from 1.378 to 1.404 Å [16] for phenylboronic acid. These bond lengths were observed at 1.365–1.393 Å and 1.365–1.392 Å [20] and calculated at 1.391–1.404 Å [28] for the 4-chloro and 4-bromophenylboronic acid molecules. These bond lengths are also calculated in the range of 1.387–1.410 Å for 2-fluorophenylboronic acid [35] and from 1.384 to 1.407 Å for 2,3-difluorophenylboronic acid [36]. In this study, the C–C bond lengths were calculated in the range of 1.390–1.404 Å for monomer and dimer structures of TC conformer of 3BrPBA.

Typical B–O bond lengths are generally ca. 1.360 Å [49] consistent with relatively strong π -interactions. These bond lengths are observed at 1.362 and 1.378 Å for phenylboronic acid [16], at 1.343 and 1.366 Å for 3-fluorophenylboronic acid molecule [18] and at 1.359 and 1.372 Å for 4-bromophenylboronic acid molecule [20]. Also in the previous work, B–O distances including for different forms were calculated at 1.366 Å and 1.373 Å for 3,4-dichlorophenylboronic acid [31]. This distance were presented from 1.371 to 1.375 Å and 1.365–1.373 Å, for the 2,4- and 2,6-dimethoxyphenylboronic acid molecule, respectively [32,33]. The optimized B–O bond lengths were obtained nearly at 1.360 Å and 1.375 Å [36]. In this paper, these values are calculated at 1.366 Å and 1.372 Å (B₉–O₇ and B₉–O₈) for monomer structure, showed more consistent with experimental values and above mentioned the calculation results of literature. However they showed differences in the dimer structure, calculated at 1.351 Å and 1.391 Å (B₉–O₇ and B₉–O₈). The hydrogen atom have important role for this changes, due to they have inter and intra-molecular interaction.

The C–B bond lengths were observed at 1.553 Å (4-chloro-) and at 1.545 Å (4-bromo-) for derivatives of phenyl boronic acid [20].

Kurt [28] calculated at 1.566 Å and 1.567 Å for the same molecules, respectively. The C₆–B₁₂ bond length was slightly greater than that typically found in boroxines, indicating a weakening of this bond by the electron-withdrawing nature of the C₆–F₅ group [29]. The optimized C–B bond lengths are calculated at 1.570 Å for the 3BrPBA molecule both monomer and dimer structures in this work. The experimental values of phenylboronic acid and 3-fluorophenylboronic acid are in well coherent, observed at 1.568 Å and at 1.562 Å [16,18]. This calculated bond lengths show very good correlation with structurally similar molecules in the literature [28–33,50].

The C–X (X; F, Cl, Br ...) bond length shows a considerable increase when substituted (X) in place of hydrogen atom. In international tables for crystallography the C–Br bond lengths values are 1.895 Å for 4-bromophenylboronic acid [20], 1.897 Å and 1.904 Å for 5-bromo salicylic acid [51]. The bond distance C–Br was calculated at 1.917 Å (monomer) and 1.916 Å (dimer) for 5-bromo salicylic acid molecule [52]. Kurt [28] calculated the C–Br bond of 4-bromophenylboronic acid at 1.917 Å using B3LYP/6-311G++(d,p) basis sets. In our present paper, this bond (C–Br) is calculated at 1.921 Å for monomer and dimer structures by using B3LYP/6-311G++(d,p) basis set, showing good coherent related paper.

The ring C–C–C bond angles were calculated at 118.1–121.3°, observed in the range of 117.2–121.8° for phenylboronic acid [16] and from 117.6° to 123.9° for 3-fluorophenylboronic acid [18], which is the good correlation (except one or two) with the normal values (120.0°) of the six-membered phenyl ring. However the C₂–C₁–C₆ and C₃–C₄–C₅ bond angle deviated from normal value smaller than the others, it can be attached B(OH)₂ group and bromine atom. The C–B–O and O–B–O bond angles of the studied molecule are different in the TT and CC conformers according to TC and

CT conformers. The hydrogen atoms (attached oxygen atoms) have important role for these disparity. The hydrogen atoms have *trans-cis* or *cis-trans* orientation for TC and CT conformers. But the hydrogen atoms of the other two conformers are the same orientation as *trans-trans* and *cis-cis* (see Table S1). The B–O–H bond angles are calculated in the range of 112.5–116.6° for all conformers. All calculated bond angles showed the small difference between the experimental values this can be due to calculation belongs to gases phase and experimental results belong to solid phase. One can quite easily see from Table S1, all the calculations of bond angles are in very consistency with the compared experimental values [16,18].

The experimental results show that the $-\text{B}(\text{OH})_2$ group is twisted by 21.4°, 35.0°, and 38.14°, relative to the ring group for phenylboronic acid [16] and 26.3° and 26.9° for 4ClPBA and 4BrPBA [20]. The corresponding calculated values are different from these values ($=0^\circ$), because both the ring and the $\text{B}(\text{OH})_2$ groups lie in the same plane (C_s point group symmetry).

Vibrational spectral analysis

The 3BrPBA molecule which has C_s point group symmetry has 16 atoms and 42 fundamental vibrational modes TC and TT conformers and C_1 point group symmetry for CT and CC conformers. Because of the imaginary frequencies, the calculations showed that the conformers CT and CC are unstable conformers in C_s point group symmetry. However, TC and TT are stable in C_s point group symmetry. Due to the C_s point group symmetry 42 fundamental vibrational modes are represented by symmetry species $29A' + 13A''$, with the A' representing in-plane motions and A'' representing out-of plane motions. The calculated wavenumbers of the most stable conformer of TC monomer and its dimer structures are tabulated in Tables 2 and S2 together with the experimental wavenumbers. A detailed description of the normal modes are performed at the B3LYP level with the triple split valence basis set 6-311++G(d,p), on the basis of relative intensities, line shape and TED given in Table 2.

In order to acquire the spectroscopic signature of the title molecule, performed a wavenumber calculation analysis by using DFT/B3LYP/6-311G++(d,p) basis set [42]. The calculated wavenumbers are usually higher than the experimental ones; this inconsistency can be a consequence of the anharmonicity and the general tendency of the quantum chemical methods to overestimate the force constants at the exact equilibrium geometry. The other possibility is the calculations have been made for free molecule in gases phase, while experiments were performed for solid sample. This discrepancy partly fixed with the scaling factor [43]. The theoretical (with the scaling factor) and experimental infrared and Raman spectra are graphed in Figs. 3 and 4 for comparative purpose for monomer and dimer structures, where the calculated intensity is plotted against harmonic vibrational wavenumbers.

The goal of this part of the work is the assignment of the vibrational absorptions to make a comparison with the results obtained from the theoretical calculations (monomer and dimer) and the structurally similar molecules. The interpretations include the ring vibrational modes and between the ring and substituent modes. To provide utility to characterize in IR and Raman spectra some strong frequencies are used, such as the stretching and bending vibrational modes; OH, CH, CC, BO, CB, CBr and CCH, BOH, CCC, CBO, CCB, CCB_r respectively, and ring torsion modes, assigned out-of plane bending of C–H and O–H of captain molecule as follows.

$\text{B}(\text{OH})_2$ vibrations

The O–H stretching modes of boronic acids in the solid state absorb broadly near 3300–3200 cm^{-1} and are extremely sensitive to formation of hydrogen bonding. The assignment O–H stretching

vibrations are pure and apprehensible. These bands were observed at 3280 cm^{-1} in IR (phenylboronic acid) [15], at 3276, 3249 cm^{-1} and at 3276, 3164 cm^{-1} in FT-IR (4-chloro-) and at 3175, 3106 and 3108 cm^{-1} in FT-Raman (4-bromophenylboronic acid) [28], at 3467 cm^{-1} in FT-IR (2-fluorophenylboronic acid) [35], at 3443, 3397 cm^{-1} in FT-IR, at 3480, 3440 cm^{-1} in FT-Raman (3,4-dichlorophenylboronic acid) [30], and at 3465, 3425 cm^{-1} in FT-IR (3,5-dichlorophenylboronic acid) [34], at 3480, 3339 cm^{-1} in FT-IR, and 3335 cm^{-1} in FT-IR (2,4-dimethoxyphenylboronic acid) [32], at 3278 cm^{-1} in FT-Raman (2,6-dimethoxyphenylboronic acid) [33] were assigned, which is typical for O–H bonded hydroxyl groups. In the prior work, we recorded this band at 3400 and 3332 cm^{-1} in FT-IR spectrum and predicted at 3685 and 3692 cm^{-1} for 2,3-difluorophenylboronic acid [36]. These vibration modes of the 3BrPBA molecule are observed at 3270 cm^{-1} in FT-IR spectrum and predicted at 3724 cm^{-1} ($\text{O}_8\text{--H}_{10}$) and 3685 ($\text{O}_7\text{--H}_{11}$) and not occurred in FT-Raman in the current study. These bands were computed at 3711, 3711 cm^{-1} ($\text{O}_8\text{--H}_{10}$) and 3471, 3443 cm^{-1} ($\text{O}_7\text{--H}_{11}$) for dimer structure. We can say; due to the inter-molecular effect the modes were showed downshift. As discussed in literature, [28–31,35,36,52] with halogens (F, Cl, Br, etc.) substitution, O–H stretching vibrations shift to a higher wavenumber region [53].

The main OH in-plane bending modes are predicted at 524, 962 and 1008 cm^{-1} (ν_{12} , ν_{21} and ν_{24}) and OH out-of-plane bending (ν_{10} , ν_{11} and ν_{13}) are computed at 447, 468, and 561 cm^{-1} for 3BrPBA molecule. This band at 583 cm^{-1} in FT-Raman and at 449 and 592 cm^{-1} in FT-IR band is assigned. As we can see from the dimer structure; the OH bending modes especially in-plane bending modes are increasing, due to the intermolecular and intramolecular interactions. Theoretical values of OH bending vibrations are good coherent in experimental values and in literature [28–31,35,36,52].

The B–O stretching modes were very intense and should also include the asymmetric stretching vibrations which are located at 1350 cm^{-1} in the infrared spectrum for phenylboronic acid [15] and at 1375 cm^{-1} for the phenylboronic acid linkage [54]. The $\nu_{\text{B--O}}$ stretching vibrations were recorded at 1373 and 1361 cm^{-1} by Kurt [28] for 4-chlorophenylboronic acid and 4-bromophenylboronic acid, respectively. For 2-fluorophenylboronic acid, this band was observed at 1385 cm^{-1} in FT-IR and at 1370 cm^{-1} in FT-Raman spectra [35]. Also this band was assigned around at 1370 cm^{-1} as the $\nu_{\text{B--O}}$ stretching vibrations for the homo- and hetero tri-nuclear boron complexes by Vargas et al. [55]. The $\nu_{\text{B--O}}$ stretching vibrations were observed at 1352 in FT-IR and at 1351, 1389 cm^{-1} in FT-Raman. These modes were calculated at 1345, 1371 and 1002 cm^{-1} by using B3LYP method which assigned as two symmetric and asymmetric modes for derivative of the phenylboronic acid [36]. In this paper, calculated B–O stretching modes at 1355 and 1339 cm^{-1} were assigned as asymmetric and symmetric modes, respectively. The B–O asymmetric and symmetric stretching bands were observed at 1377 and 1346 cm^{-1} in FT-Raman and FT-IR spectra, respectively. There is downshift effect in the BO symmetric modes while higher shift in the BO asymmetric modes from monomeric to dimeric structures.

The C–B stretching modes (between ring and $\text{B}(\text{OH})_2$ group) evaluate for ring derivatives of boronic acids. The bands were assigned at 1089 and 1085 cm^{-1} in the spectra of the normal and deuterated phenylboronic acids, and at 1084 cm^{-1} for diphenyl phenylboronate to the C–B stretching modes by Faniran et al. [15]. Kurt observed at 1303 cm^{-1} in FT-Raman for 4-bromophenylboronic acid and computed at 1320 cm^{-1} by using B3LYP/6-311++G(d,p) [28]. This vibration was observed at 802 cm^{-1} as medium bands in FT-IR, shifted negatively by ca. 280 cm^{-1} due to the chlorine substitution for 3,5 dichlorophenylboronic acid molecule [30]. The C–B stretching vibrations were saved at 1345, 899, 635 cm^{-1} for 2,3 difluorophenylboronic acid, observed at 1352

Table 2

The comparison of the calculated harmonic frequencies and experimental (FT-IR and FT-Raman) wavenumbers (cm^{-1}) using by B3LYP method 6-311++G(d,p) basis set for monomer and dimer structures of TC conformer of 3BrPBA.

Modes no	Sym. species	Theoretical/monomer		Theoretical/dimer		Experimental		TED ^b ($\geq 10\%$) Monomer
		Unscaled freq.	Scaled freq. ^a	Unscaled freq.	Scaled freq. ^a	FT-IR	FT-Raman	
v1	A''	12	11	41, 19	40, 18		9m	τ CBCO (96)
v2	A'	116	114	165, 146	162, 144		98vs	δ CCB (47), δ CBO (14), δ CCBr (24)
v3	A''	122	120	131, 129	129, 127		118s	τ CCCB (35), τ CBCH (14), τ CCCB (14), τ COCB (11)
v4	A''	178	175	181, 181	177, 177		177vs	γ CBr [τ CCCB (39), τ CBrCH (21)]
v5	A'	245	241	272, 259	267, 255		272w	δ CCBr (37), δ CCO (29)
v6	A'	297	292	301, 298	296, 293		308s	vCB (43), δ CCBr (24)
v7	A'	341	336	368, 353	361, 347			δ CBO (35), vCB (19), δ CCC (15), vCB (10)
v8	A''	403	396	402, 397	395, 390	402m	386m	τ CCCC (39), τ CCCH (26), γ OH (17)
v9	A'	444	436	456, 446	448, 439			δ CBO (33), δ CCB (20)
v10	A''	455	447	455, 450	447, 442	449s		γ OH (37) [τ BOOH (19), τ CBOH (18)], τ CCCC (12)
v11	A''	476	468	478, 477	470, 469			γ OH (63) [τ BOOH (29), τ CBOH (34)], τ CCCC (12)
v12	A'	533	524	589, 550	579, 540	510m	516vw	δ BOH (45), δ CCC (16)
v13	A''	571	561	786, 737	773, 724	592m	583w	γ OH (79) [τ BOOH (41), τ CBOH(38)]
v14	A''	666	654	657, 656	645, 645	646s		τ CCCC (30)
v15	A'	671	660	673, 672	662, 660	665s	666s	τ BOOH (15), δ CCC (15), τ COCB (10), τ CCCC (12)
v16	A''	717	705	717, 716	705, 704	700vs	702vw	τ CCCH (38), τ COCB (22), τ CCCC (16), τ CBOH (10)
v17	A'	774	761	779, 775	766, 762	764s	774vw	δ CCC (22), vCB (19), vCB (13), vBO (12), vCC (10)
v18	A''	806	793	808, 807	794, 794	792vs	800vw	γ CH (78)
v19	A''	886	871	885, 884	870, 869	836m		γ CH (84)
v20	A''	943	927	943, 943	927, 927	904s	915vw	γ CH (91)
v21	A'	979	962	1005, 994	988, 977			δ BOH (64) vCB (21)
v22	A''	1007	990	1007, 1007	990, 990			γ CH (98)
v23	A'	1011	994	1014, 1012	997, 995	994s	996vs	δ CCC (42), vCC (32)
v24	A'	1025	1008	1200, 1064	1180, 1046			δ BOH (78), vBO (19)
v25	A'	1087	1068	1096, 1085	1077, 1067	1033vs	1074m	vCC (56), δ CC (14)
v26	A'	1112	1093	1117, 1113	1098, 1095			vCC (42), δ CC (35)
v27	A'	1136	1117	1175, 1129	1155, 1110	1124s	1134w	vCC (30), δ CC (17), δ BOH (13)
v28	A'	1197	1176	1197, 1195	1176, 1175	1190s	1172vw	δ CC (73), vCC (16)
v29	A'	1294	1272	1294, 1291	1272, 1269	1260vw	1264vw	vCC (67), δ CC (22)
v30	A'	1337	1315	1340, 1338	1317, 1315			δ CC (69), vCC (15)
v31	A'	1362	1339	1357, 1328	1334, 1306	1346vs		vBO sym. ((28), vCB (25), δ BOH (16), δ CC (11)
v32	A'	1378	1355	1404, 1403	1381, 1380		1377vw	vBO asym. (63), vCC (12)
v33	A'	1438	1414	1452, 1445	1428, 1421	1404vs	1404vw	vCC (27), δ CC (24), vBO asym. ((17)
v34	A'	1506	1480	1507, 1506	1481, 1481	1478s	1482vw	δ CC (56), vCC (30)
v35	A'	1593	1566	1594, 1593	1567, 1566	1558s	1558m	vCC (68), δ CC (18)
v36	A'	1629	1601	1629, 1629	1602, 1602	1595s	1598s	vCC (68), δ CC (14)
						1702vw		Overtone + combination
						1799w		Overtone + combination
						1829vw		Overtone + combination
						1884vw		Overtone + combination
						1953vw		Overtone + combination
						2249vw		Overtone + combination
						2366w		Overtone + combination
						2430w		Overtone + combination
v37	A'	3162	3029	3159, 3159	3027, 3027		3028vw	vCHasym. (99)
v38	A'	3172	3039	3172, 3172	3039, 3039			vCHasym. (100)
v39	A'	3195	3061	3195, 3195	3061, 3061		3063s	vCHasym. (100)
v40	A'	3202	3068	3202, 3202	3068, 3068		3092vw	vCHsym. (100)
v41	A'	3847	3685	3623, 3594	3471, 3443	3270vs		vOH (100) (O_7-H_{11})
v42	A'	3887	3724	3874, 3873	3711, 3711			vOH (100) (O_8-H_{10})

^a Wavenumbers in the ranges from 4000 to 1700 cm^{-1} and lower than 1700 cm^{-1} are scaled with 0.958 and 0.983 for B3LYP/6-311++G(d,p) basis set, respectively.

^b v; Stretching, γ ; out-of plane bending, δ ; in-plane-bending, τ ; torsion, ρ ; scissoring, ϕ ; twisting, Γ ; rocking, vw; very weak, w; weak, m; medium, s; strong, vs; very strong.

and 1351 cm^{-1} in FT-IR and FT-Raman, respectively, in well agreement [36]. We also determined C–B stretching modes at 1339 cm^{-1} (1346 cm^{-1} in FT-IR), 962 cm^{-1} , 761 cm^{-1} (764 cm^{-1} in FT-IR) for 3BrPBA. These means that C–B vibrations are sensitive for halogens like chlorine, fluorine, bromine, etc. substitution.

The B–O–H bending and torsion modes of with the ring and boronic acid groups (except for identified as OH/CH in plane and out-of plane) are speared and mixed the other modes were assigned by TED if anyone see pursuit Table 2. The OH or related the interaction modes are different with the each other in the monomer and dimer structures of the title molecule. This showed that inter- or intra- molecular interactions are important for these type molecules.

Phenyl ring vibrations

Stretching modes. The presence of the C–H stretching vibrations the multiple peaks seem in the 3000–3100 cm^{-1} range which is the characteristic region for these modes. The C–H in plane bending vibration appears in the range of 1000–1300 cm^{-1} and C–H out-of-plane bending vibration seem in the range of 750–1000 cm^{-1} [56]. These modes were discussed in literature [28,30,31,36] predicted in the range of ca. 3030–3100 cm^{-1} for similar compounds. The C–H stretching modes were computed in the range of 3029–3068 cm^{-1} for monomer and 3027–3068 cm^{-1} for dimer structures by using the B3LYP/6-311++G(d,p) method and observed at 3028, 3063 and 3092 cm^{-1} in FT-Raman for 3BrPBA molecule. All modes of CH stretching are very pure see TED contribution (ca. 100%).

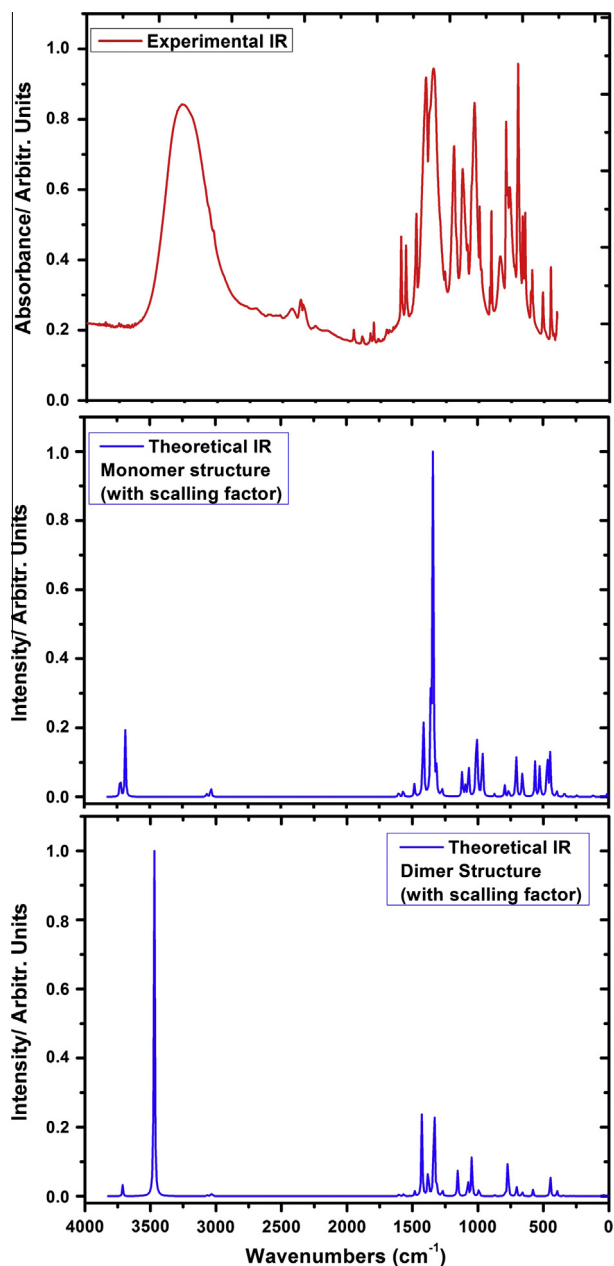


Fig. 3. The experimental and calculated monomer and dimer structures (with the scale factor) infrared spectra of the 3BrPBA.

The CC stretching modes are also the other highly characteristic and very much important for the aromatic ring, showed in the region 1625–1430 cm^{-1} . Varsanyi [57] gave that the bands were of variable intensity and were observed at 1625–1590, 1590–1575, 1540–1470, 1465–1430 and 1380–1280 cm^{-1} from the frequency ranges for the five bands. The assignments of five bands in IR spectra of C–C stretching vibrations of phenylboronic acid were assigned in the range of 1620–1320 cm^{-1} [15]. Similarly, the C–C stretching modes were recorded in the range of 1590–1010 cm^{-1} and 1588–1004 cm^{-1} in FT-IR and FT-Raman for 4-bromophenylboronic acid and 1596–1060 cm^{-1} and 1588–1085 cm^{-1} in FT-IR and FT-Raman for 4-chlorophenylboronic acid [28], in the range of 1617–1034 cm^{-1} (IR) for 2-fluorophenylboronic acid [35], supported with DFT calculations computed ca. 1650–990 cm^{-1} using B3LYP calculations [28,30,31,36]. The C–C stretching vibrations were calculated 1629–1465 cm^{-1} , 1304–1213 cm^{-1} , 1149–1063 cm^{-1} , 899 cm^{-1} ,

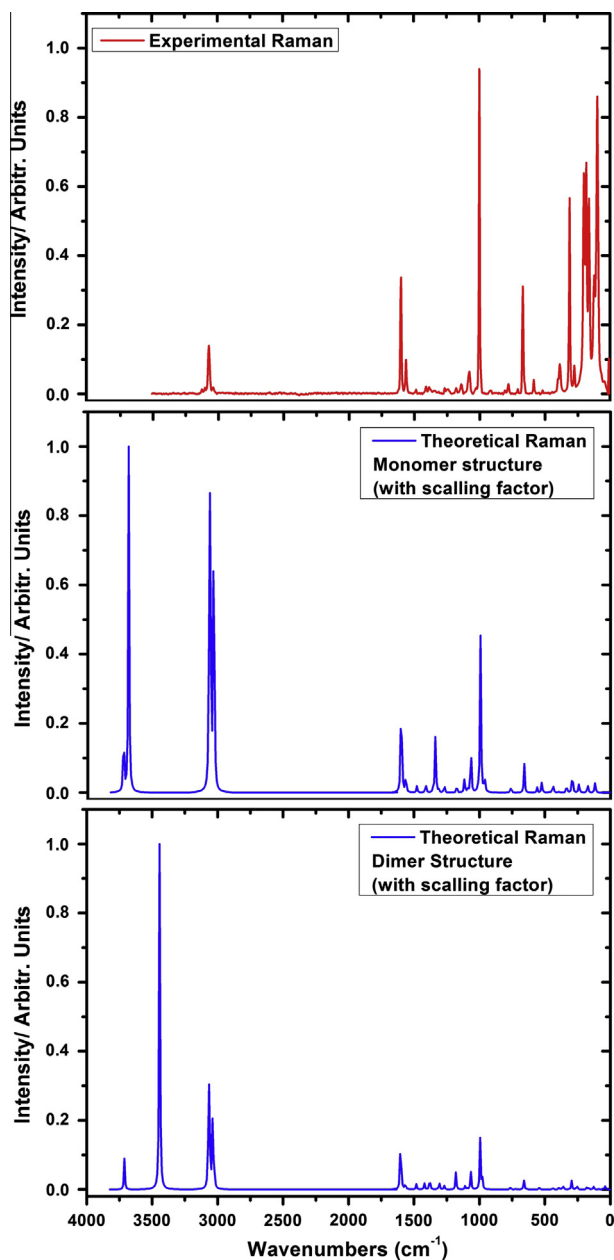


Fig. 4. The experimental and calculated monomer and dimer structures (with the scale factor) Raman spectra of the 3BrPBA.

and 635 cm^{-1} by B3LYP method and observed between 1628, 1266, 1214, 1154 cm^{-1} in FT-IR and 1626, 1590, 1474, 1292, 1269, 1215, 1148 and 1065 cm^{-1} in FT-Raman for 2,3-difluorophenylboronic acid [36]. In the present study, the CC stretching modes are computed at 1601–1355, 1315–1068, and 994 cm^{-1} for monomer TC conformer of the title molecule, by using the hybrid B3LYP level of theory in DFT with the 6-311++G(d,p) basis set, showed very well correlation with the observed in the range of 1595–1404, 1260–1033, and 994 cm^{-1} in FT-IR and 1598–1377, 1172–1074 and 996 cm^{-1} in FT-Raman, respectively. The dominant C–C stretching vibrations are calculated at 1601 and 1566 cm^{-1} , appeared pure modes with the TED contribution 68%. The modes of dimer structure of the 3BrPBA molecule are showed parallel results except some small deviations.

The theoretical wavenumbers of C–Br stretching vibration coupled with other group vibrations. According to TED, there is no pure C–Br band vibration. In the bromine compounds, the C–Br

stretching mode appears at longer wavelength region 200–480 cm^{-1} as reported by Varsanyi [57]. In previous study, in FT-Raman spectrum of 5-bromo salicylic acid [52], the band at 283 cm^{-1} is assigned to C–Br stretching vibration coupled with ring deformation. The theoretical wavenumber of this band at 285 cm^{-1} coincides well with the experimental one. The C–Br stretching vibration modes were computed for 4-bromophenylboronic acid at 547 and 389 cm^{-1} by using B3LYP method and not observed in FT-IR or FT-Raman spectra [28]. We recorded the mode of the C–Br at 308 cm^{-1} in FT-Raman and theoretically calculated at 292 cm^{-1} showing well agreement with the literature and experimental result. There is not any big difference between the monomer and dimer structures of the molecule.

Bending, torsion and other ring modes. The C–H in-plane bending vibrations are calculated very wide range nearly 1601–1068 cm^{-1} , observed at 1595, 1558, 1478, 1404, 1346, 1260, 1190, 1124, and 1033 cm^{-1} in FT-IR and 1598, 1558, 1482, 1404, 1264, 1172, 1134, and 1074 cm^{-1} in FT-Raman. The C–H out of plane bending modes are assigned ν_{22} , and ν_{20-18} , predicted at 990, 927, 871, and 793 cm^{-1} , respectively. The out of plane bending modes were observed at 904, 836, and 792 cm^{-1} in FT-IR, at 915 and 800 cm^{-1} in FT-Raman. The TED contributions showed that the out-of plane modes have been also highly pure modes like the in-plane bending fundamental. Both the in-plane and out-of plane bending vibrations are contaminated other modes, especially CC stretching modes. The results showed very good correlation for monomer and dimer structures of the studied molecule. We also look at the literature, theoretical and experimental data for the similar compounds, our results show very good correlation [28–31,35,36,52].

The most contribution CCC bending mode is observed at 994 and 996 cm^{-1} in FT-IR and in FT-Raman, calculated wavenumbers of this mode coincides at 994 cm^{-1} after scaling. The ring deformation, torsion modes are obtained in a large region and contaminated other modes and determined as out-of plane modes of C–H or O–H. Therefore, these modes will not be discussed here. The TEDs of these vibrations are aggregated and evaluated this part.

The C–Br in-plane bending and out-of-plane bending modes appear in variable region according to molecular structure and state of the bromine substituent. The C–Br in plane bending vibrations are calculated at 292, 241 and 114 cm^{-1} which are assigned to 308, 272 and 98 cm^{-1} in FT-Raman. The C–Br out-of-plane bending vibration is assigned to 177 cm^{-1} in FT-Raman, which shows excellent agreement with calculated value (175 cm^{-1}). This is in agreement with the literature data [28,52,57,58]. The remainder bending and torsion modes of the related bromine atom accounted in Table 2.

To see the correlations of infrared and Raman are graphed one by one as Fig. S2a and b. Also to evaluate the harmony of between the calculated and experimental wavenumbers are plotted correlation graphics and given in Fig. S3. As can be seen from Fig. S3, the experimental fundamentals have a better correlation with the theoretical results. To see the relations between the calculated and experimental wavenumbers are usually linear and described by the following equations:

$$\nu_{\text{cal}} = 1.0350\nu_{\text{exp}} - 26.555 \quad (\text{Total: } R^2 = 0.9946)$$

$$\nu_{\text{cal}} = 0.9593\nu_{\text{exp}} - 51.802 \quad (\text{Infrared} - R^2 = 0.9967)$$

$$\nu_{\text{cal}} = 1.0141\nu_{\text{exp}} - 30.532 \quad (\text{Raman} - R^2 = 0.9971)$$

NMR spectra

The chemical shift analysis is one of the most important techniques for the structural analysis for organic compounds. We preferred the useful and common technique for chemical shifts to have more information about the studied molecule. Therefore, ^1H

and ^{13}C NMR analysis of 3BrPBA molecule were evaluated both experimentally and theoretically. The experimental ^1H and ^{13}C NMR spectra of the title molecule are given in Fig. S4(a) and (b), respectively. The experimental and theoretical ^1H and ^{13}C chemical shifts in DMSO solution are gathered in Table 3 for monomer and dimer structures. The atom positions are listed according to Fig. 1.

Firstly, full geometry optimization of 3BrPBA is obtained B3LYP/6-311G++(d,p) basis set. After then, ^1H and ^{13}C NMR calculations of the steady compound are performed by using GIAO and 6-311++G(d,p) basis set IEFPCM/DMSO solution. The GIAO [46,47] approach to molecular systems was substantially evolved by an efficient application of the method to the ab-initio SCF calculations, by using techniques taken from analytic derivative methodology. To calculate the isotropic chemical shifts δ with respect to tetramethylsilane values were used (TMS) $\delta_{\text{iso}}^{\text{X}} = \sigma_{\text{iso}}^{\text{TMS}} - \sigma_{\text{iso}}^{\text{X}}$.

The 3BrPBA molecule has four hydrogen atoms as attached to the ring, and two hydrogen atoms attached the oxygen atoms of $\text{B}(\text{OH})_2$ group. The chemical shifts of aromatic protons of organic molecules are usually observed in the range of 7.00–8.00 ppm. However, the proton chemical shift of organic molecules varies greatly with the electronic environment of the proton. Hydrogen attached or nearby electron-withdrawing atom or group can decrease the shielding and move the resonance of attached proton toward to a higher frequency, whereas electron-donating atom or group increases the shielding and moves the resonance toward to a lower frequency [59,60]. Attached to ring protons are accumulated this range experimentally see in Table 3, and Fig. S4a. Theoretical isotropic chemical shifts of protons are calculated (monomer) at 8.15, 7.75, 7.70, 7.54, 4.93 and 4.15 ppm, experimental values are recorded in the region 7.95–7.96, 7.77–7.87, 7.58–7.59, 7.55–7.56, 7.23–7.27 and 2.49–2.51 ppm. The chemical shifts are calculated at 8.23, 8.20, 7.84, 7.78, 7.65, and 5.12 ppm for dimer structure. All results of the proton NMR are increasing from monomer to dimer form of the molecule. Especially H_{10} and H_{11} of chemical shifts were showed more rising the other. This can be due to the changed the electronic environment. The chemical shift of H_{12} and H_{15} are higher than the other protons. H_{10} and H_{11} of chemical shift of proton are smaller than the other (especially H_{10}). These mean that the electronic charge density around of these atoms can be effected the influence of rapid proton exchange, hydrogen bond, solvent effect, etc. in the molecular system.

Generally, aromatic carbons give resonances in overlapped areas of the spectrum with chemical shift values from 100 to 150 ppm [61,62]. There are six different carbon atoms, which are

Table 3

Experimental and theoretical, ^1H and ^{13}C NMR isotropic chemical shifts (with respect to TMS) of 3BrPBA with DFT (B3LYP 6-311++G(d,p)) method in DMSO.

Hydrogen atoms	B3LYP 6-311++G(d,p)		
	Exp.	Monomer	Dimer
H(10)	2.49–2.51	4.93	5.12
H(11)	7.23–7.27	4.15	8.20
H(12)	7.95–7.96	8.15	8.23
H(13)	7.55–7.56	7.54	7.65
H(14)	7.77–7.87	7.75	7.84
H(15)	7.58–7.59	7.70	7.78
Carbon atoms	B3LYP 6-311++G(d,p)		
	Exp.	Monomer	Dimer
C(1)	122.13	137.00	137.64
C(2)	136.15	140.68	140.52
C(3)	137.02	145.93	146.40
C(4)	133.36	139.99	140.23
C(5)	130.26	134.51	134.81
C(6)	133.19	139.22	139.31

attached phenyl ring and consistent with the structure on basis of molecular symmetry of the present molecule. The ^{13}C NMR chemical shifts of our title molecule are observed and calculated this range, showing good coherent with the each other. The chemical shifts of the carbon atoms (from C_1 to C_6) of the 3BrPBA molecule were calculated at 137.00, 140.68, 145.93, 139.99, 134.51 and 139.22 ppm, which observed at 122.13, 136.15, 137.02, 133.36, 130.26 and 133.19 ppm, respectively. C_1 atom has smaller chemical shifts than the other ring carbon atoms, due to shielding effect which the non-electronegative property of $\text{B}(\text{OH})_2$ group. Moreover, taking a glance at the literature the results of chemical shift of the molecule are showed very good correlation for the similar molecules [35–37]. The value of C_3 atom has the biggest one, because of the electronegative feature of the bromine atom. The dimer results of the molecule are showed same correlation for carbon chemical shifts.

Fig. S5 demonstrates the correlation graphics between the experimental and theoretical total chemical shifts of the title molecule. The relations between the calculated and experimental chemical shifts (δ_{exp}) are usually linear and described by the following equation:

$$\delta_{\text{cal}} (\text{ppm}) = 1.0587\delta_{\text{exp}} - 0.3350 \quad (\text{Total: } R^2 = 0.9980)$$

The performances of the B3LYP method with respect to the prediction of the relative shielding within the molecule are nearly close. Based on the ^1H and ^{13}C chemical shifts data collected in Table 3 one can deduce that qualitatively the ^{13}C and ^1H NMR chemical shifts of 3BrPBA are described fairly well. However, the small deviation between experimental and computed chemical shifts of these protons may be due to the presence of intermolecular hydrogen bonding.

Electronic properties

UV-Vis spectrum and frontier molecular orbital analysis

The UV-Vis (electronic absorption) spectrum of 3BrPBA molecule is measured in ethanol and water at room temperature experimentally and optimized geometry in the ground state are obtained in the framework of TD-DFT calculations with the B3LYP/6-311++G(d,p) method (IEFPCM method). Because of the TD-DFT calculations to predict the electronic absorption spectra is a quite reasonable method. TD-DFT methods are computationally more expensive than semi-empirical methods but allow easily studies of medium size molecules [63]. The calculated electronic values, such as absorption wavelengths (λ), excitation energies (E), oscillator strengths (f), and major contributions of the transitions and assignments of electronic transitions and experimental absorption wavelengths (energies) are accumulated in Table 4 in two solvents (monomer and dimer structure of TC form). The experimental and theoretical UV-Vis spectra of the studied molecule were shown in Fig. S6. The maximum absorption values are 222.57 and 274.36 nm in ethanol and 222.57 and 274.02 nm in water solution and the calculated values are signed at ca. 257, 234 and 227 nm by TD-DFT/B3LYP/6-311++G(d,p) basis set both two solutions. The calculated dimer results are at ca. 258 and 235 nm for these solvents.

Highest occupied molecular orbital (HOMO) and the lowest unoccupied molecular orbital (LUMO) orbitals are also called FMOs as they lie at the outermost boundaries of the electrons of the molecules. The ability of electron giving and accepting characterizes for HOMO and LUMO, respectively. Their properties help for physicists and chemists for the main orbital taking part in chemical reaction. This is also used by the frontier electron density for predicting the most reactive position in π -electron systems and also explains several types of reaction in conjugated system [64]. The conjugated molecules are determined by a small HOMO–LUMO

Table 4
Experimental and calculated wavelengths λ (nm), excitation energies (eV), oscillator strengths (f) of 3BrPBA molecule gas phase, in ethanol and water solutions for monomer and dimer structure of TC conformer.

λ (nm)	E (eV)	f	Assignments	Major contributes	λ (nm)	E (eV)
<i>Monomer structure</i>						
TD-DFT/B3LYP/6-311++G(d,p) gas phase						
260.04	4.7685	0.0211	$\pi-\pi^*$	H \rightarrow L (78%), H - 1 \rightarrow L + 1 (13%)	-	-
236.91	5.2340	0.0000	$\pi-\pi^*$	H \rightarrow L + 2 (85%), H \rightarrow L + 3 (13%)	-	-
227.41	5.4527	0.0428	$\pi-\pi^*$	H \rightarrow L + 1 (54%), H - 1 \rightarrow L (35%), H \rightarrow L (10%)	-	-
TD-DFT/B3LYP/6-311++G(d,p) in ethanol						
257.70	4.8117	0.0279	$\pi-\pi^*$	H \rightarrow L (78%), H - 1 \rightarrow L + 1 (13%)	274.36	4.5196
234.06	5.2978	0.0000	$\pi-\pi^*$	H \rightarrow L + 2 (94%)	-	-
227.09	5.4603	0.0571	$\pi-\pi^*$	H \rightarrow L + 1 (48%), H - 1 \rightarrow L (40%), H \rightarrow L (11%)	222.57	5.5713
TD-DFT/B3LYP/6-311++G(d,p) in water						
257.55	4.81455	0.0272	$\pi-\pi^*$	H \rightarrow L (77%), H - 1 \rightarrow L + 1 (13%)	274.02	4.5252
233.87	5.30201	0.0000	$\pi-\pi^*$	H \rightarrow L + 2 (94%)	-	-
226.96	5.46343	0.0562	$\pi-\pi^*$	H \rightarrow L + 1 (47%), H - 1 \rightarrow L (40%), H \rightarrow L (11%)	222.57	5.5713
<i>Dimer structure</i>						
TD-DFT/B3LYP/6-311++G(d,p) gas phase						
260.57	4.7588	0.0467	$\pi-\pi^*$	H \rightarrow L (43%), H - 1 \rightarrow L + 1 (36%)		
260.45	4.7610	0.0000	$\pi-\pi^*$	H - 1 \rightarrow L (42%), H \rightarrow L + 1 (36%)		
238.86	5.1914	0.0003	$\pi-\pi^*$	H - 1 \rightarrow L + 1 (44%), H \rightarrow L (42%)		
TD-DFT/B3LYP/6-311++G(d,p) in ethanol						
258.09	4.8045	0.0580	$\pi-\pi^*$	H \rightarrow L (42%), H - 1 \rightarrow L + 1 (36%)		
258.03	4.8056	0.0000	$\pi-\pi^*$	H - 1 \rightarrow L (42%), H \rightarrow L + 1 (36%)		
235.47	5.2660	0.0007	$\pi-\pi^*$	H - 1 \rightarrow L + 1 (51%), H \rightarrow L (49%)		
TD-DFT/B3LYP/6-311++G(d,p) in water						
257.93	4.80745	0.0564	$\pi-\pi^*$	H \rightarrow L (42%), H - 1 \rightarrow L + 1 (36%)		
257.87	4.80855	0.0000	$\pi-\pi^*$	H - 1 \rightarrow L (42%), H \rightarrow L + 1 (36%)		
235.35	5.26881	0.0007	$\pi-\pi^*$	H - 1 \rightarrow L + 1 (51%), H \rightarrow L (49%)		

H: HOMO, L:LUMO.

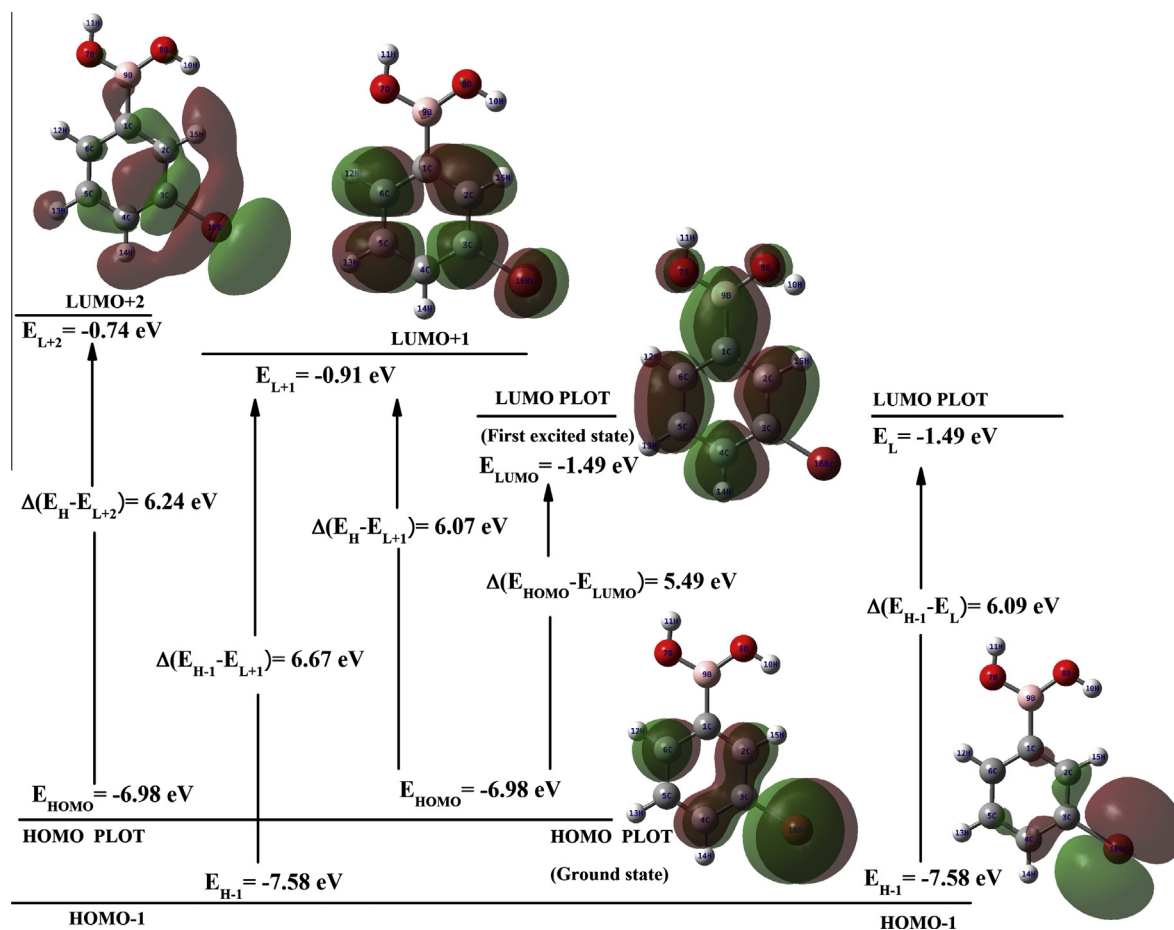


Fig. 5. The selected frontier molecular orbitals of 3BrPBA with the energy gaps.

separation, which is the result of a significant degree of intra-molecular charge transfer from the end-capping electron-donor groups to the efficient electron-acceptor group through- π -conjugated path [65].

To understand the bonding scheme of present molecule the frontier orbitals FMOs ($H-1 \rightarrow L$, $H \rightarrow L$, $H \rightarrow L+1$, $H \rightarrow L+2$, $H-1 \rightarrow L+1$ and $H-1 \rightarrow L+2$ orbital) are pictured in Fig. 5. The nodes of HOMO orbital placed on the ring and bromine atom. But the nodes of LUMO orbital placed symmetrically all over the molecule except for hydrogen attached to oxygen. The positive phase is red and the negative one is green. The main HOMO a charge density localized over the bromine atom and ring group of the current molecule. However the charge of bromine atom alternated $B(OH)_2$ group from HOMO to LUMO of 3BrPBA molecule. The HOMO and LUMO and FMOs energy gap explains the eventual charge transfer interactions taking place within the molecule. The FMOs energy calculated by B3LYP/6-311++G(d,p) method for gas phase, ethanol and water solutions: $E_{HOMO} = -6.98$ eV, $E_{LUMO} = -1.49$ eV and the energy gap $E_{HOMO-LUMO} = 5.49$ eV.

The energy gaps ($H-1 \rightarrow L$, $H \rightarrow L$, $H \rightarrow L+1$, $H \rightarrow L+2$, $H-1 \rightarrow L+1$ and $H-1 \rightarrow L+2$ orbital) are calculated 6.09, 5.49, 6.07, 6.24, 6.61, 6.67 and 6.84 eV, respectively for gas phase for the title molecule (see Table 5). These values are calculated (monomer and dimer structures) in two solvents and presented in Table 5. The value of chemical hardness is 2.75 eV in gas phase 2.78 eV in ethanol and 2.79 eV in water solvents for monomer structure. The chemical hardness (h) and electronegativity (χ) are increasing 0.01 eV in solvents from ethanol to water in monomer structure. The value of electrophilicity index (ω) is the same in two solvents as 3.25 eV (monomer) and 3.24 eV (dimer).

All values are gathered in Table 5 both monomer and dimer structures of TC conformer of the title molecule.

Total, partial, and overlap population density-of-states

The TDOS, PDOS, and OPDOS (or COOP) density of states [66–68] are calculated and generated by convoluting the molecular orbital information with Gaussian curves of unit height and FWHM of 0.3 eV using the GaussSum 2.2 program [48] in point of the Mulliken population analysis. In the boundary region, neighboring orbitals may show quasi degenerate energy levels. To provide a pictorial representation of MO (molecule orbital) compositions and their contributions to chemical bonding, the density of state of the molecule (TDOS, PDOS and OPDOS) are graphed and given in Figs. 6–8, respectively. The COOP diagram shows the bonding, anti-bonding and nonbonding nature of the interaction of the two orbitals, atoms or groups. The positive and negative values indicate a bonding interaction and an anti-bonding interaction and zero value indicates nonbonding interactions, respectively [69]. Additionally, the OPDOS diagram allows us to the determination and comparison of the donor-acceptor properties of the ligands and ascertains the bonding, non-bonding.

The PDOS mainly presents the composition of the fragment orbitals contributing to the molecular orbitals. The HOMO orbitals are localized on the C_6H_4 group and bromine atom (64% + 35% = 99%) and $B(OH)_2$ (a bit O_7 atom) group (1%), while LUMO orbitals spread on the C_6H_4 and $B(OH)_2$ group (81% + 19% = 100%). To say bonding and anti-bonding properties is difficult of the molecule according to percentage sharing of atomic orbitals or molecular fragments in the molecule. The OPDOS diagram and some of its orbitals of energy values of inter-

Table 5
The calculated energies values and the energy gaps of 3BrPBA molecule using by the TD-DFT/B3LYP method using 6-311++G(d,p) basis set for monomer and dimer structures of TC conformer.

TD-DFT/B3LYP 6-311++G(d,p)	Monomer			Dimer		
	Gas	Ethanol	Water	Gas	Ethanol	Water
E_{total} (Hartree)	-2981.937937	-2981.94604	-2981.946432	-5963.891125	-1015.35763	-1015.358305
E_{HOMO} (eV)	-6.98	-7.03	-7.04	-7.01	-7.20	-7.20
E_{LUMO} (eV)	-1.49	-1.47	-1.47	-1.55	-1.44	-1.44
E_{HOMO-1} (eV)	-7.58	-7.56	-7.56	-7.01	-7.20	-7.20
E_{LUMO+1} (eV)	-0.91	-0.90	-0.90	-1.51	-1.41	-1.41
E_{LUMO+2} (eV)	-0.74	-0.66	-0.66	-0.95	-0.65	-0.65
E_{LUMO+3} (eV)	-0.37	-0.27	-0.26	-0.95	-0.65	-0.65
$E_{HOMO-1-LUMO}$ gap (eV)	6.09	6.09	6.09	5.46	5.76	5.76
$E_{HOMO-LUMO}$ gap (eV)	5.49	5.56	5.57	5.46	5.76	5.76
$E_{HOMO-LUMO+1}$ gap (eV)	6.07	6.13	6.14	5.50	5.79	5.79
$E_{HOMO-LUMO+2}$ gap (eV)	6.24	6.37	6.38	6.06	6.55	6.55
$E_{HOMO-LUMO+3}$ gap (eV)	6.61	6.76	6.78	6.06	6.55	6.55
$E_{HOMO-1-LUMO+1}$ gap (eV)	6.67	6.66	6.66	5.50	5.79	5.79
$E_{HOMO-1-LUMO+2}$ gap (eV)	6.84	6.90	6.90	6.06	6.55	6.55
Chemical hardness (h)	2.75	2.78	2.79	2.73	2.88	2.88
Electronegativity (χ)	4.24	4.25	4.26	4.28	4.32	4.32
Chemical potential (μ)	-4.24	-4.25	-4.26	-4.28	-4.32	-4.32
Electrophilicity index (ω)	3.27	3.25	3.25	3.36	3.24	3.24

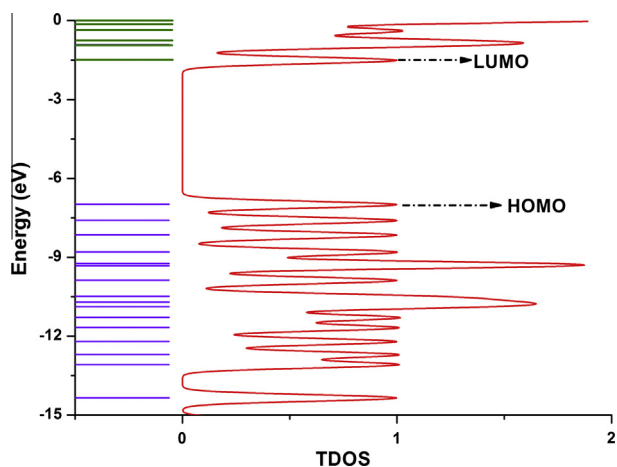


Fig. 6. The total electronic density of states diagram of the 3BrPBA.

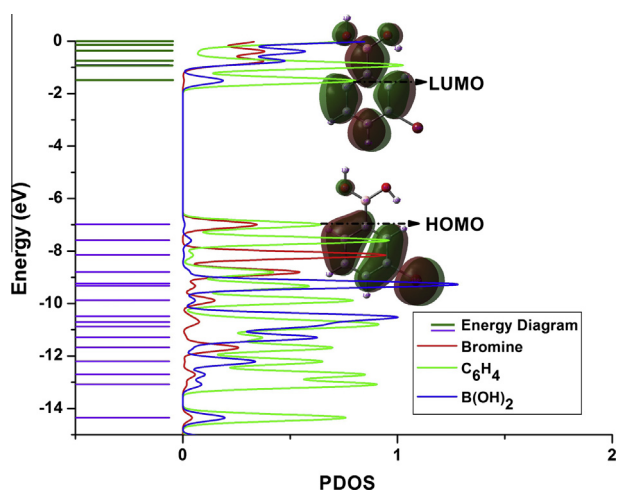


Fig. 7. The partial electronic density of states diagram of the 3BrPBA.

action between selected groups which are shown from figure easily, C_6H_4 group \leftrightarrow $B(OH)_2$ group (blue line) system is negative and positive (anti-bonding and bonding interaction) also C_6H_4

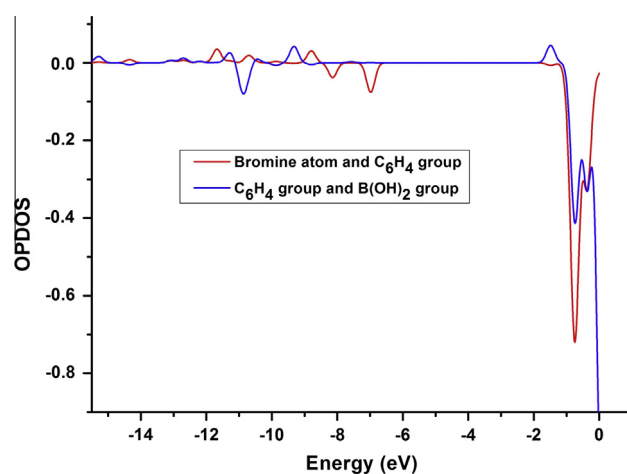


Fig. 8. The overlap population electronic density of states OPDOS diagram of the 3BrPBA.

group \leftrightarrow bromine atom (red line) showed the same trend. As can be seen from the OPDOS plots for the title molecule have anti-bonding (negative range) character in frontier HOMO and LUMO molecular orbitals for C_6H_4 group and bromine atom.

Molecular electrostatic potential surface

To map onto the constant electron density surface, the MEPs of molecules are plotted. It is superimposed on top of the total energy density as a shell. The MEPs generally showed that the maximum positive region which preferred site for nucleophilic attack symptoms as blue color, while the maximum negative region which preferred site for electrophilic attack indications as red color. Because of the usefulness feature to study reactivity given that an approaching electrophile will be attracted to negative regions (where the electron distribution effect is dominant). The MEPs simultaneously exhibits molecular size, shape as well as positive, negative and neutral electrostatic potential regions in terms of color grading and is very useful in research of molecular structure with its physicochemical property relationship [70,71].

The MEPs of 3BrPBA molecule in 3D and 2D contour plots are represented in Fig. 9. The values of the electrostatic potential at the surface are illustrated by different colors for different data in the map of MEPs. The potential rises from red to blue color. The

colors line up in the range of -0.0104 a.u. (dark red) and 0.0104 a.u. (dark blue) in this compound. The blue and red colors represent strongest attraction and repulsion, respectively. The MEPs map of 3BrPBA showed that while regions having the positive potential are near OH groups, the regions having the negative potential are over the oxygen atoms (O_7 and O_8). From these results, we can say that near the H_{10} and H_{11} atoms indicate the strongest attraction and the oxygen atoms (O_7 and O_8) indicate the strongest repulsion (see Fig. 9). The sliced 2D MEPs contour map of the title molecule provides more exhaustive information regarding molecular electrostatic potential distribution, by showing the values in an assortment of spatial site around the molecule. The 2D MEPs are pictured in the molecular plane of the studied molecule. The around of the oxygen atoms have been electron rich region and all the around of hydrogen atoms correspond to the electron deficient region. The maximum values of negative and positive potential corresponding to the nucleophilic and electrophilic region are -0.02 a.u. and 0.4 a.u. respectively.

Mulliken atomic charges

The computed atomic charges in the reactive display an important role in the application of quantum mechanical calculations the molecular system. We calculated the Mulliken atomic charges of 3BrPBA by using the DFT/B3LYP method 6-311++G(d,p) basis set. The results of Mulliken atomic charges of monomer and dimer structures of the title molecule and phenyl boronic acid are reported and compared. The computed Mulliken atomic charges are gathered in Table 6. The substitution of the aromatic ring by bromine atoms leads to a redistribution of electron density. The charge distribution of $B(OH)_2$ group is showed the same charge (negative or positive) with the phenylboronic acid, however, the charges of the aromatic ring of the molecules show different charge with each other. For example, the charge of C_3 atom is negative charge in phenyl boronic acid, however, because of added bromine atom, the value of Mulliken atomic charge shows positive charge in our molecule. While C_2 and C_6 atoms are positive charge in phenyl boronic acid and negative in the current molecule. Hydrogen atoms exhibit a positive charge, which is an acceptor atoms both two molecules. The Mulliken atomic charges of monomer and dimer

Table 6

Comparison of Mulliken charges of phenylboronic acid and monomer and dimer structures of 3BrPBA molecule by using B3LYP/6-311++G(d,p) basis set.

Atoms	PBA	3-BrPBA/monomer	3-BrPBA/dimer
C1	-0.688	-0.570	-0.488
C2	0.205	-0.231	-0.008
C3	-0.350	0.340	0.288
C4	-0.015	-0.057	-0.078
C5	-0.457	-0.229	-0.243
C6	0.211	-0.140	-0.309
O7	-0.365	-0.378	-0.579
O8	-0.359	-0.363	-0.553
B9	0.523	0.548	0.634
H10	0.232	0.226	0.259
H11	0.286	0.289	0.521
H12	0.195	0.174	0.164
H13	0.160	0.183	0.187
H14	0.160	0.200	0.200
H15	0.108	0.196	0.176
Br16/H16	0.155	-0.187	-0.172

structure of the 3BrPBA molecule are showed similar distributions. However the bromine atom replaced the H_{16} showed as a negative charge. The results also are the same trend for the prior work for also derivatives of the phenyl boronic acid [36].

Thermodynamic properties

The zero-point vibrational energy, thermal energy, specific heat capacity, rotational constants, entropy and dipole moment of TC form of the current molecule are computed and listed in Table 7 at room temperature (at 298.15 K) in the ground state by using DFT/B3LYP/6-311++G(d,p) method both C_1 and C_s symmetry point groups.

To view depending on the temperature change for the thermodynamic functions (heat capacity (C) entropy (S) and enthalpy changes (H)) the temperature gradually increased ranging from 100 K to 700 K, varied every 50 K. The statically thermodynamic functions: C, S and H changes for the heading molecule are achieved from the theoretical harmonic frequencies and listed in Table 8 according to vibrational analysis. It is concluded that the

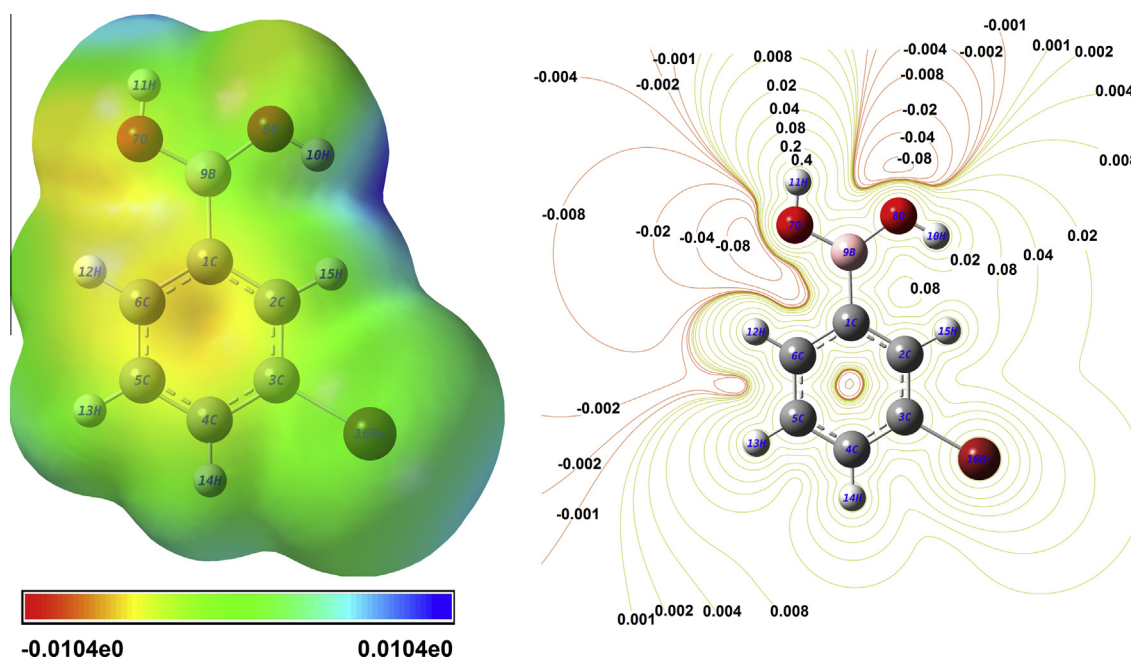


Fig. 9. The molecular electrostatic potential 3D map and 2D contour map for 3BrPBA molecule.

Table 7
The calculated thermo dynamical parameters of 3BrPBA at 298.15 K for all conformers in ground state at the B3LYP/6-311++G(d,p) level for C₁ and C_s symmetry point groups.

Conformers	Trans–Cis	Cis–Trans	Trans–Trans	Cis–Cis
<i>C₁ symmetry</i>				
SCF energy (a.u.)	–2981.937959	–2981.937876	–2981.9351	–2981.932603
Zero point vib. energy (kcal mol ^{–1})	71.85052	71.78158	71.61785	71.89308
Rotational constants (GHz)	1.95499	1.91815	1.94165	1.90003
	0.44523	0.45209	0.45091	0.44575
	0.36292	0.36602	0.36593	0.36861
Specific heat, C _v (cal mol ^{–1} K ^{–1})	34.592	34.644	34.947	34.535
Entropy, S (cal mol ^{–1} K ^{–1})	98.736	99.685	98.140	97.937
Dipole moment (debye)	0.6753	2.8609	3.8253	2.7188
Imaginary frequencies	–	–	–	–
<i>C_s symmetry</i>				
SCF energy (a.u.)	–2981.93793685	–2981.93787654	–2981.9351	–2981.93128100
Zero point vib. energy (kcal mol ^{–1})	71.78072	71.73558	71.67394	71.4549
Rotational constants (GHz)	1.95678	1.91830	1.94149	1.93013
	0.44523	0.45218	0.45095	0.44803
	0.36270	0.36592	0.36595	0.36362
Specific heat, C _v (cal mol ^{–1} K ^{–1})	34.659	32.689	34.881	33.155
Entropy, S (cal mol ^{–1} K ^{–1})	100.528	92.810	97.927	93.343
Dipole moment (debye)	0.6225	2.8660	3.8218	2.8712
Imaginary frequencies	–	1 (–15.17 cm ^{–1})	–	1 (–80.86 cm ^{–1})

Table 8
Thermodynamic properties at different temperatures at the B3LYP/6-311++G(d,p) level for 3BrPBA.

T (K)	C (cal mol ^{–1} K ^{–1})	S (cal mol ^{–1} K ^{–1})	H (kcal mol ^{–1})
100	14.606	73.438	1.221
150	19.571	81.095	2.174
200	24.701	87.998	3.380
250	29.841	94.507	4.843
298.15	34.659	100.527	6.492
300	34.839	100.755	6.560
350	39.543	106.790	8.520
400	43.847	112.621	10.706
450	47.709	118.247	13.096
500	51.133	123.664	15.668
550	54.157	128.872	18.402
600	56.827	133.874	21.277
650	59.192	138.676	24.279
700	61.298	143.289	27.391

thermodynamic functions are increasing with temperature, due to the fact that the molecular vibrational intensities increase with temperature. Also the correlation graphics of these are graphed in Fig. 10. The correlation equations between heat capacity,

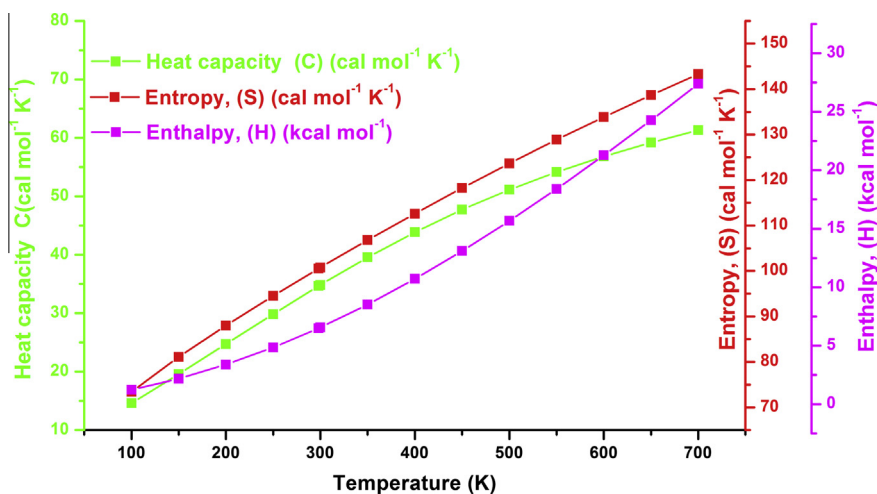


Fig. 10. The correlation graphic of heat capacity, entropy, enthalpy and temperature for 3BrPBA molecule.

entropy, enthalpy changes and temperatures are fitted by quadratic formulas and the corresponding fitting factors (R^2) for these thermodynamic properties are 0.9996, 0.9999 and 0.9998, respectively. The corresponding fitting equations are as follows:

$$C = 1.4702 + 0.1314T - 6.5256 \times 10^{-5} T^2 \quad (R^2 = 0.9996)$$

$$S = 57.0205 + 0.1530T - 4.6888 \times 10^{-5} T^2 \quad (R^2 = 0.9999)$$

$$H = -0.5670 + 0.0121T + 4.0258 \times 10^{-5} T^2 \quad (R^2 = 0.9998)$$

The thermodynamic data help to useful information for the further study on 3BrPBA. To compute the other thermodynamic energies according to relationships of thermodynamic functions and estimate directions of chemical reactions according to the second law of thermodynamics in Thermochemical field, the results of thermodynamic calculations can be used.

Nonlinear optical properties and dipole moment

This part of the study includes electronic dipole moment, molecular polarizability, anisotropy of polarizability and molecular first hyperpolarizability of 3BrPBA molecule. To obtain polarizability and hyperpolarizability tensors (α_{xx} , α_{xy} , α_{yy} , α_{xz} , α_{yz} , α_{zz} and β_{xxx} ,

Table 9

The dipole moments μ (D), the polarizability α (a.u.), the average polarizability α_0 ($\times 10^{-24}$ esu), the anisotropy of the polarizability $\Delta\alpha$ ($\times 10^{-24}$ esu), and the first hyperpolarizability β ($\times 10^{-33}$ esu) of 3BrPBA.

μ_x	0.5433	β_{xxx}	746.6912
μ_y	0.3039	β_{xxy}	-398.7837
μ_z	0.0000	β_{xyy}	339.0549
μ_0	0.6226	β_{yyy}	230.5103
α_{xx}	22.030127	β_{xxz}	0.0000
α_{xy}	0.599084	β_{xyz}	0.0000
α_{yy}	17.235044	β_{yyz}	0.0000
α_{xz}	0.000000	β_{xzz}	-193.9547
α_{yz}	0.000000	β_{yzz}	140.0338
α_{zz}	9.343303	β_{zzz}	0.0000
α_{total}	16.202825	β_x	891.7912976
$\Delta\alpha$	39.73780912	β_y	-28.2395719
		β_z	0.0000000
		β	892.2383044

$\beta_{xxy}, \beta_{xyy}, \beta_{yyy}, \beta_{xxx}, \beta_{xxy}, \beta_{xyy}, \beta_{xzz}, \beta_{yzz}, \beta_{zzz}$ are used a frequency job output file of Gaussian. However, the units of α and β values of Gaussian output are in atomic units (a.u.) therefore they have been converted into electronic units (esu) (for α ; 1 a.u. = 0.1482×10^{-24} esu, for β ; 1 a.u. = 8.6393×10^{-33} esu). The mean polarizability (α), anisotropy of polarizability ($\Delta\alpha$) and the average value of the first hyperpolarizability (β) can be calculated using the equations.

$$\alpha_{tot} = \frac{1}{3}(\alpha_{xx} + \alpha_{yy} + \alpha_{zz})$$

$$\Delta\alpha = \frac{1}{\sqrt{2}} \left[(\alpha_{xx} - \alpha_{yy})^2 + (\alpha_{yy} - \alpha_{zz})^2 + (\alpha_{zz} - \alpha_{xx})^2 + 6\alpha_{xz}^2 + 6\alpha_{xy}^2 + 6\alpha_{yz}^2 \right]^{\frac{1}{2}}$$

$$\langle\beta\rangle = \left[(\beta_{xxx} + \beta_{xxy} + \beta_{xzz})^2 + (\beta_{yyy} + \beta_{yyz} + \beta_{yxx})^2 + (\beta_{zzz} + \beta_{zxx} + \beta_{zyy})^2 \right]^{\frac{1}{2}}$$

The parameters described above and electronic dipole moment $\{\mu_i$ ($i = x, y, z$) and total dipole moment μ_{tot} for 3BrPBA molecule are gathered and listed in Table 9. The total dipole moment can be calculated using the following equation.

$$\mu_{tot} = \left(\mu_x^2 + \mu_y^2 + \mu_z^2 \right)^{\frac{1}{2}}$$

It is well known that the higher values of dipole moment, molecular polarizability, and hyperpolarizability are important for more active NLO properties. 3BrPBA has relatively homogeneous charge distribution and it does not have large dipole moment. The calculated value of dipole moment is found to be 0.6226 D. The highest value of dipole moment is observed for component μ_x . In this direction, this value is equal to 0.5433 D and μ_z is the smallest one as zero. The calculated polarizability and anisotropy of the polarizability of the title molecule are $16.202825 \times 10^{-24}$ and $39.73780912 \times 10^{-24}$ esu, respectively. The magnitude of the first hyperpolarizability β , is one of important key factors in a NLO system. The B3LYP/6-311++G(d,p) calculated first hyperpolarizability value (β) of 3BrPBA is equal to $892.2383044 \times 10^{-33}$ esu. If we compare the common values of urea; the first hyperpolarizability, polarizability and anisotropy of the polarizability values of 3BrPBA are larger than those of urea.

Conclusions

The present study is off to illuminate the spectroscopic properties of derivative of phenylboronic acid. The FT-IR, FT-Raman UV-Vis, ^1H and ^{13}C NMR techniques are used both experimentally and theoretically, to identify frequency assignments, magnetic and electronic properties for monomeric and dimeric structures of 3BrPBA molecule. The optimized geometric parameters (bond lengths and bond angles) are theoretically determined at B3LYP/

6-311++G(d,p) level (monomer and dimer) and, compared with the similar molecules. The vibrational (FT-IR and FT-Raman) spectra of 3BrPBA are recorded with experimental and computed vibrational wavenumbers and TED. The magnetic properties of the studied molecule are observed and calculated. The electronic properties are calculated and the experimental electronic spectra are recorded with help of UV-Vis spectrometer. The molecular orbitals, MEPs contour/surface drawn and the electronic transitions identified for UV-Vis spectra may lead to the understanding of properties and dynamics of the molecule. The MEPs shows the negative potential sites are on oxygen atoms as well as the positive potential sites are around the hydrogen (H_{10} and H_{11}) atoms. The thermodynamic functions; heat capacity, entropy and enthalpy changes increase with the increasing temperature owing to the intensities of the molecular vibrations increase with increasing temperature. The polarizability, anisotropy of polarizability and first hyperpolarizability of 3BrPBA molecule are presented. All calculated results compared with experimental ones show an acceptable general agreement.

Appendix A. Supplementary material

Supplementary data associated with this article can be found, in the online version, at <http://dx.doi.org/10.1016/j.molstruc.2014.07.058>.

References

- [1] E. Frankland, B.F. Duppa, *Justus Liebigs Annalen der Chem* 115 (3) (1860) 319–322.
- [2] N.A. Petasis, *Aust. J. Chem.* 60 (2007) 795–798.
- [3] P.C. Trippier, C. McGuigan, *Med. Chem. Commun.* 1 (2010) 183–198.
- [4] E. Cuthbertson, *Boronic Acids: Properties and Applications*, Alfa Aesar, Heysham, 2006.
- [5] D.G. Hall, In *Boronic Acids*, first ed., Wiley-VCH, Weinheim, 2005.
- [6] M.M. Reichvilser, C. Heinzl, P. Klüfers, *Carbohydr. Res.* 345 (2010) 498–502.
- [7] M.R. O'Donovan, C.D. Mee, S. Fenner, A. Teasdale, D.H. Phillips, *Mutat. Res.* 724 (2011) 1–6.
- [8] J.N. Cambre, B.S. Sumerlin, *Polymer* 52 (2011) 4631–4643.
- [9] M.R. Stabile, W.G. Lai, G. DeSantis, M. Gold, J.B. Jones, *Bioorg. Med. Chem. Lett.* 21 (1996) 2501–2506.
- [10] P.R. Westmark, B.D. Smith, *J. Pharm. Sci.* 85 (1996) 266–269.
- [11] X. Chen, G. Liang, D. Whitmire, J.P. Bowen, *J. Phys. Org. Chem.* 11 (1988) 378–386.
- [12] W. Tjarks, A.K.M. Anisuzzaman, L. Liu, S.H. Soloway, R.F. Barth, D.J. Perkins, D.M. Adams, *J. Med. Chem.* 35 (1992). 16228–11633.
- [13] Y. Yamamoto, *Pure Appl. Chem.* 63 (1991) 423–426.
- [14] F. Alam, A.H. Soloway, R.F. Barth, N. Mafune, D.M. Adam, W.H. Knoth, *J. Med. Chem.* 32 (1989) 2326–2330.
- [15] J.A. Faniran, H.F. Shurvell, *Can. J. Chem.* 46 (1968) 2089–2095.
- [16] S.J. Rettig, J. Trotter, *Can. J. Chem.* 55 (1977) 3071–3075.
- [17] M.K. Cyrański, A. Jezierska, P. Klimentowska, J.J. Panek, A. Sporzynski, *J. Phys. Org. Chem.* 21 (2008) 472–482.
- [18] Y.M. Wu, C.C. Dong, S. Liu, H.J. Zhu, Y.Z. Wu, *Acta Cryst. E62* (2006) o4236–o4237.
- [19] P.R. Cuamatzi, H. Tlahuext, H. Höpfl, *Acta Cryst. E65* (2009) o44–o45.
- [20] M.R. Shimpi, N.S. Lekshmi, V.R. Pediretti, *Cryst. Growth Des.* 7 (10) (2007) 1958–1963.
- [21] B. Zarychta, J. Zaleski, A. Sporzynski, M. Dabrowski, J. Serwatowski, *Acta Cryst. C60* (2004) o344–o345.
- [22] A. Vega, M. Zarate, H. Tlahuext, H. Höpfl, *Acta Cryst. E66* (2010) o1260.
- [23] D. Sajana, L. Joseph, N.V.M. Karabacak, *Spectrochim. Acta A* 81 (2011) 85–98.
- [24] P.J. Stephens, F.J. Devlin, C.F. Chabalowski, M.J. Frisch, *J. Phys. Chem.* 98 (1994) 11623–11627.
- [25] F.J. Devlin, J.W. Finley, P.J. Stephens, M.J. Frish, *J. Phys. Chem.* 99 (1995) 16883–16902.
- [26] S.Y. Lee, B.H. Boo, *Bull. Korean Chem. Soc.* 17 (1996) 760–764.
- [27] G. Rauhut, P. Pulay, *J. Phys. Chem.* 99 (1995) 3093–3100.
- [28] M. Kurt, *J. Raman Spectrosc.* 40 (2009) 67–75.
- [29] M. Kurt, *J. Mol. Struct.* 874 (2008) 159–169.
- [30] S. Ayyappan, N. Sundaraganesan, M. Kurt, T.R. Sertbakan, M. Ozduran, *J. Raman Spectrosc.* 41 (2010) 1379–1387.
- [31] M. Kurt, T.R. Sertbakan, M. Özduvan, M. Karabacak, *J. Mol. Struct.* 921 (2009) 178–187.
- [32] Ö. Alver, C. R. Chimie 14 (2011) 446–455.
- [33] Ö. Alver, C. Parlak, *Vib. Spectrosc.* 54 (2010) 1–9.
- [34] M. Kurt, T.R. Sertbakan, M. Özduvan, *Spectrochim. Acta A* 70 (2008) 664–673.

- [35] Y. Erdogdu, M.T. Gulluoglu, M. Kurt, *J. Raman Spectrosc.* 40 (2009) 1615–1623.
- [36] M. Karabacak, E. Kose, A. Atac, M.A. Cipiloglu, M. Kurt, *Spectrochim. Acta A* 97 (2012) 892–908.
- [37] M. Karabacak, L. Sinha, O. Prasad, A.M. Asiri, M. Cinar, *Spectrochim. Acta A* 115 (2013) 753–766.
- [38] U. Rani, M. Karabacak, O. Tanrıverdi, M. Kurt, N. Sundaraganesan, *Spectrochim. Acta A* 92 (2012) 67–77.
- [39] P. Hohenberg, W. Kohn, *Phys. Rev.* 136 (1964) B864–B871.
- [40] A.D. Becke, *J. Chem. Phys.* 98 (1993) 5648–5652.
- [41] C. Lee, W. Yang, R.G. Parr, *Phys. Rev. B* 37 (1988) 785–789.
- [42] M.J. Frisch et al., GAUSSIAN 09, Revision A.1, Gaussian Inc., Wallingford, CT, 2009.
- [43] N. Sundaraganesan, S. Ilakiamani, H. Salem, P.M. Wojciechowski, D. Michalska, *Spectrochim. Acta A* 61 (2005) 2995–3001.
- [44] J. Baker, A.A. Jarzecki, P. Pulay, *J. Phys. Chem. A* 102 (1998) 1412–1424.
- [45] P. Pulay, J. Baker, K. Wolinski, 2013 Green Acres Road, Suite A, Fayetteville, AR 72703, USA.
- [46] R. Ditchfield, *J. Chem. Phys.* 56 (1972) 5688–5691.
- [47] K. Wolinski, J.F. Hinton, P. Pulay, *J. Am. Chem. Soc.* 112 (1990) 8251–8260.
- [48] N.M. O'Boyle, A.L. Tenderholt, K.M. Langner, *J. Comp. Chem.* 29 (2008) 839–845.
- [49] P.N. Horton, M.B. Hursthouse, M.A. Becket, M.P.R. Hankey, *Acta Cryst. E Struct. Rep.* E60 (2004) o2204–o2206.
- [50] K.L. Bhat, N.J. Howard, H. Rostami, J.H. Lai, Charles W. Bock, *J. Mol. Struct. (Theochem.)* 723 (2005) 147–157.
- [51] Z. Liu, Y. Qu, M. Tan, H. Zhu, *Acta Cryst. E* 60 (2004) 01310–01311.
- [52] M. Karabacak, M. Kurt, *J. Mol. Struct.* 919 (2009) 215–222.
- [53] L.J. Bellamy, *The Infrared Spectra of Complex Molecules*, Wiley, New York, 1959.
- [54] G. Kahraman, O. Beskarcler, Z.M. Rzave, E. Piskin, *Polymer* 45 (2004) 5813–5828.
- [55] G. Vargas, I. Hernandez, H. Höpfl, M. Ochoa, D. Castillo, N. Farfan, R. Santillan, E. Gomez, *Inorg. Chem.* 43 (2004) 8490–8500.
- [56] M. Silverstein, G. Clayton Basseler, C. Morill, *Spectrometric Identification of Organic Compounds*, Wiley, New York, 2001.
- [57] G. Varsanyi, *Assignments of Vibrational Spectra of Seven Hundred Benzene Derivatives*, 1–2, Adam Hilger, 1974.
- [58] N. Sundaraganesan, H. Saleem, S. Mohan, M. Ramalingam, V. Sethuraman, *Spectrochim. Acta A* 62 (2005) 740–751.
- [59] N. Subramania, N. Sundaraganesan, J. Jayabharathi, *Spectrochim. Acta A* 76 (2010) 259–269.
- [60] A. Coruh, F. Yilmaz, B. Sengez, M. Kurt, M. Cinar, M. Karabacak, *Struct. Chem.* 22 (2011) 45–56.
- [61] H.O. Kalinowski, S. Berger, S. Braun, *Carbon-¹³NMR spectroscopy*, John Wiley & Sons, Chichester, 1988.
- [62] K. Pihlaja, E. Kleinpeter (Eds.), *Carbon-13 Chemical Shifts in Structural and Stereochemical Analysis*, VCH Publishers, Deerfield Beach, 1994.
- [63] J. Fabian, *Dyes Pigments* 84 (2010) 36–53.
- [64] K. Fukui, T. Yonezawa, H. Shingu, *J. Chem. Phys.* 20 (1952) 722–725.
- [65] C.H. Choi, M. Kertesz, *J. Phys. Chem.* 101A (1997) 3823–3831.
- [66] R. Hoffmann, *Solids and Surfaces: A Chemist's View of Bonding in Extended Structures*, VCH Publishers, New York, 1988.
- [67] T. Hughbanks, R. Hoffmann, *J. Am. Chem. Soc.* 105 (1983) 3528–3537.
- [68] J.G. Malecki, *Polyhedron* 29 (2010) 1973–1979.
- [69] M. Chen, U.V. Waghmare, C.M. Friend, E. Kaxiras, *J. Chem. Phys.* 109 (1998). 6854–6880.
- [70] J.S. Murray, K. Sen, *Molecular Electrostatic Potentials, Concepts and Applications*, Elsevier, Amsterdam, 1996.
- [71] E. Scrocco, J. Tomasi, in: P. Lowdin (Ed.), *Advances in Quantum Chemistry*, Academic Press, New York, 1978.